TORSIONAL RIGIDITY OF WOOD COMPOSITE I-JOISTS

Daniel Hindman†

Assistant Professor
Department of Wood Science and Forest Products
Virginia Polytechnic Institute and State University
Brooks Forest Products Center
1650 Ramble Road
Blacksburg, VA 24061-0503

Harvey B. Manbeck

Distinguished Professor Emeritus
Agricultural and Biological Engineering
Pennsylvania State University
210 Agricultural and Biological Engineering Building
University Park, PA 16802

and

John J. Janowiak†

Professor
School of Forest Resources
Pennsylvania State University
307 Forest Resources Laboratory
University Park, PA 16802

(Received March 2004)

ABSTRACT

The torsional rigidity of I-joists is useful in determining the lateral torsional buckling of unsupported beams, the stiffness of two-way floor systems, and the natural frequency for wood floors. The torsional rigidity of two I-joist materials, one manufactured with laminated veneer lumber (LVL) flanges and the other with laminated strand lumber (LSL) flanges, was measured. There were no significant differences in the measured torsional rigidity of the two I-joist materials. The measured torsional rigidity terms were compared with predictions of torsional rigidity based upon the distinct cross-sectional dimensions and previously measured material elastic constants. A finite element model was used to predict the torsional rigidity of the I-joist section and to examine the effect of isotropic and orthotropic assumptions. An isotropic torsional rigidity prediction using G_{12} values of the web material and G_{13} values of the flange materials provided agreement with the measured 95% confidence intervals for both I-joist materials. Prediction of torsional rigidity was heavily influenced by the planar shear moduli in the larger cross-sectional dimension. The use of an assumed E:G ratio of 16:1 for all wood materials overpredicted the torsional rigidity values by 30% compared to more refined predictions.

Keywords: Torsional rigidity, shear modulus, wood composite I-joists, isotropic elasticity, orthotropic elasticity.

INTRODUCTION

Wood composite I-joists occupy a majority market share of floor joist production for new residential housing construction. These materials are fabricated using solid-sawn lumber or wood composite flange members connected with plywood or oriented strandboard (OSB) webs. As the size and complexity of housing increase, I-joist members are being used as continuous beams and cantilever members. No information

† Member of SWST.

Wood and Fiber Science, 37(2), 2005, pp. 292–303
© 2005 by the Society of Wood Science and Technology

about the lateral torsional stability of these materials has been found in the published literature. One of the key components to the determination of the lateral torsional stability of I-joists is the torsional rigidity (GJ) term.

This paper discusses the evaluation and prediction of GJ values from I-joist materials. Torsional rigidity measurement and prediction of I-joists are in anticipation of using these GJ values for the prediction of lateral buckling loads for unbraced beams. Similar work was also conducted to measure and predict the GJ values associated with solid-sawn lumber and structural composite lumber sections (Hindman et al. 2005a).

MATERIALS AND METHODS

Experimental study materials

The two I-joist products tested were commercially available materials from Trus Joist, a Weyerhaeuser Company. The TJI 150 I-joists have laminated veneer lumber (LVL) flanges with an OSB web. Both the LVL and OSB were composed of southern pine (*Pinus spp*) material. The TJI 120 TS I-joists have laminated strand lumber (LSL) flanges with an OSB web. The LSL was composed of yellow poplar (*Liriodendron tulipifera*), and the OSB was composed of southern pine (*Pinus spp*) strands. Table 1 describes the dimensions of the I-joists used and the maximum bending moment. Figure 1 shows the manufactured construction of the two commercial I-joist materials including the web-flange connection. Prior to test evaluation, all specimens were allowed to equilibrate under ambient laboratory conditions of 23.9°C (75°F) and 45% relative humidity, producing an equilibrium moisture content of 8.5%.

Experimental measurement of torsional rigidity

Measurement of the GJ term used a torsion test including an effective length modification discussed by Tarnopol'skii and Kincis (1985). Figure 2 shows the torsional stress analyzer (TSA) used to measure the GJ values. The TSA applied a centric torque to one end of the specimen while the other end was held rigid. A rotary actuator applied the torque, and a LeBow Model 2121−2K torque sensor with 226.0 N-m (2000 in-lb) capacity and a sensitivity of 0.23 N-m (2 in-lb) measured the applied torque. An LVDT with a 0.64-mm (0.25-in) displacement range and 0.00025 cm (0.0001-in.) sensitivity measured the change in arc length during specimen loading. Measurements of the arc length were correlated to the angle of specimen end rotation. LabView software collected data from both instruments to generate a torque vs. angle curve. Specimens were loaded until an angular rotation of two degrees was attained. Sixteen specimens of each I-joist material were tested with three loading repetitions per specimen. The gage length of both I-joist materials was 147 cm (58-in.). The web sections of the I-joist were blocked to provide full support to the cross-section at the grips.

To eliminate any potential clamping effects, an effective length determination (ELD) protocol applied a corrective virtual adjustment to the specimen gage length to account for possible clamping effect resulting from the grips of the TSA loading device. The corrective adjustment to the specimen gage length was determined by evaluating the torque-theta relationship of a series of reduced gage length specimens. The intercept of the curve of the torque-theta vs. gage length is the ELD value used to modify the mea-

TABLE 1. *Description of test I-joist materials*[1].

Material	Overall height cm (in)	Flange height cm (in) cm (in)	Flange width N-m (ft-lbs)	Maximum moment[2]
LVL I-joist[3]	24.1 (9.50)	3.81 (1.50)	3.81 (1.50)	2220 (1640)
LSL I-joist[4]	24.1 (9.50)	3.81 (1.50)	4.45 (1.75)	2088 (1540)

[1] All materials were conditioned at 23.9 C (75 degrees F) and 45% relative humidity
[2] Maximum moment is the allowable stress design value.
[3] LVL I-joist materials consisted of southern pine LVL and southern pine OSB
[4] LSL I-joist materials consisted of yellow poplar LSL and southern pine OSB

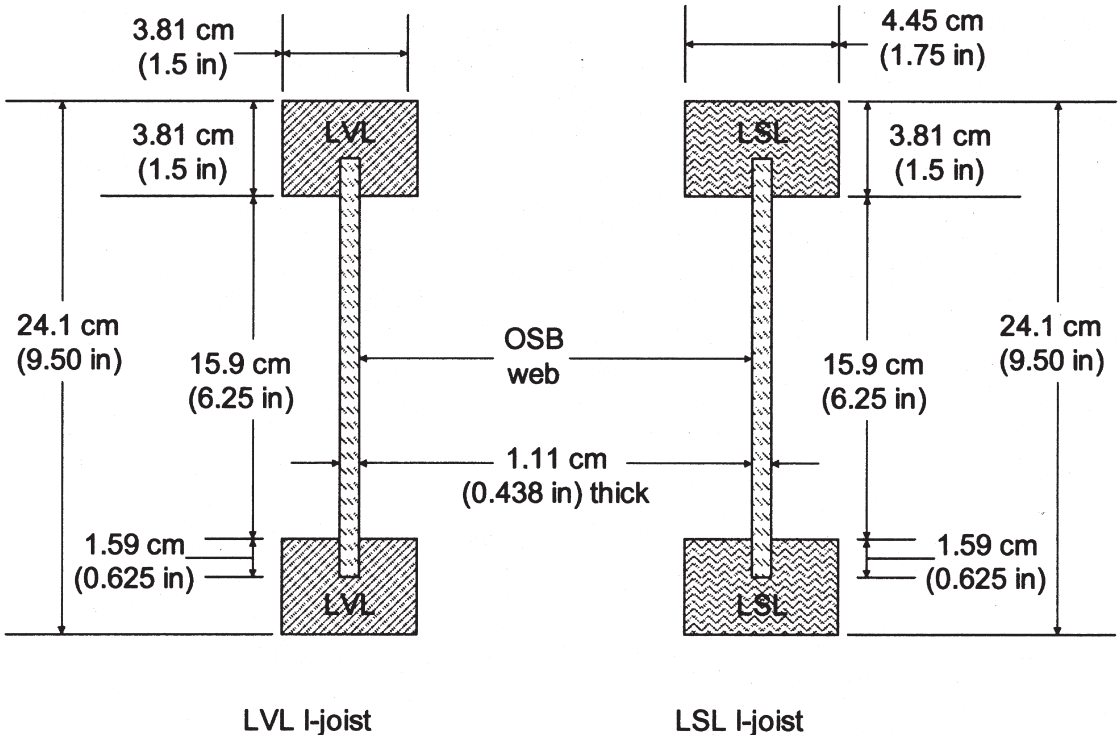

FIG. 1. Definition sketch of I-joist materials.

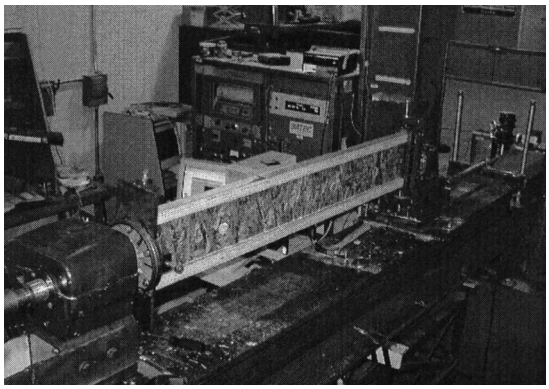

FIG. 2. Torsional stiffness analyzer (TSA).

sured gage length to form the effective length. Subsequent ELD testing included lengths of 147 cm (58 in.), 130 cm (51 in.), 99 cm (39 in.) and 76.2 cm (30 in.) length specimens.

Data reduction and calculations for the determination of torsional rigidity also followed analogous procedures to those described by Hindman (2003) from applied torque and angle measurements according to Eq. (1). The torque-angle was measured using the TSA, and the effective length term L_e is the specimen gage length modified by the ELD corrective adjustment.

$$GJ = \left(\frac{T}{\theta}\right) L_e \qquad (1)$$

where

T = applied torque
θ = resultant rotation (or angle of twist)
L_e = effective length including measured gage length and ELD adjustment

Development of torsional rigidity model

Numerical methods are required to predict the GJ term associated with non-rectangular, non-circular cross-sections, such as I-joists. Various sources including Timoshenko and Goodier (1951) and Lekhnitskii (1963) provide the generalized differential equations for torsion of a prismatic beam. Equations (2) and (3) show the

basic two-dimensional stress field equations written to describe the torsional rigidity of prismatic sections using isotropic and orthotropic elasticity assumptions, respectively. The term ϕ is the Prandtl stress function. The Prandtl stress function allows the description of the two-dimensional shear stress field by a single scalar value. The Prandtl stress function must be chosen in such a manner to satisfy equilibrium and boundary conditions. The planar shear moduli are related by the Prandtl differential terms to β, the angle of twist per unit length. Further discussion can be found in Cook and Young (1985) or other mechanics of materials textbooks.

$$\frac{\partial^2 \phi}{\partial z^2} + \frac{\partial^2 \phi}{\partial y^2} = 2G\beta \tag{2}$$

$$\frac{1}{G_{xy}} \frac{\partial^2 \theta}{\partial z^2} + \frac{1}{G_{xz}} \frac{\partial^2 \phi}{\partial y^2} = -2\beta \tag{3}$$

where

ϕ = Prandtl stress function
y, z = axes from Fig. 3
G_{xy} = in-plane shear modulus (Fig. 3)
G_{xz} = through-thickness shear modulus (Fig. 3)
β = rate of twist (degrees per length)

The finite element method is one numerical technique used to solve the two-dimensional field equations. Segerlind (1984) presents a finite element program called TDFIELD. TDFIELD contains options to customize the generalized two-dimensional field problem to a torsional analysis, heat transfer, groundwater flow, and several other engineering problems. The program is written in FORTRAN code and is capable of a maximum mesh containing 250 nodes and 300 elements.

In order to develop the element mesh for the current I-joist GJ study, a convergence study of the TDFIELD program analyzed several different rectangular cross-section sizes to determine an optimal configuration. Equations (4) and (5) show the closed form GJ solutions of isotropic and orthotropic homogenous rectangular beams,

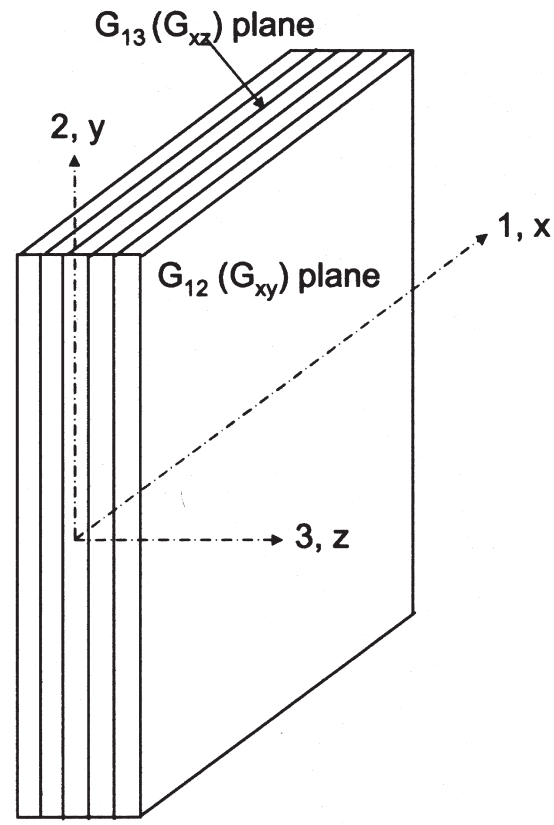

FIG. 3. Definition sketch of axes of a rectangular section.

respectively. Figure 3 shows the planar orientations of a homogenous rectangular wood composite element.

$$GJ = G_{12}\left[\frac{b^3 h}{3}\left(1 - \frac{2}{\pi}\left(\frac{b}{h}\right)\right)\right] \tag{4}$$

$$GJ = G_{12}\left[\frac{b^3 h}{3}\left(1 - \frac{192b}{\pi^5 h}\sqrt{\frac{G_{12}}{G_{13}}}\right)\right] \tag{5}$$

where

GJ = torsional rigidity of section
G_{12}, G_{13} = planar shear moduli (Fig. 3)
b = width of rectangular section
h = height of rectangular section

TABLE 2. *Properties of rectangular sections used in TDFIELD convergence study.*

Section	Width	Height	Shear modulus
Isotropic Aluminum	0.64 cm (0.25 in)	7.62 cm (3.0 in)	26.2 GPa (3.80×10^6 psi)[1]
Isotropic Wood	3.81 cm (1.5 in)	23.5 cm (9.25 in)	862 MPa (1.25×10^5 psi)
Orthotropic Wood	3.81 cm (1.5 in)	23.5 cm (9.25 in)	862 MPa (1.25×10^5 psi) for G_{12}, 616 MPa (8.93×10^4 psi) for G_{13}

[1] Aluminum shear modulus values correspond to 6061-T6 material.
[2] Wood G_{12} values were estimated assuming an E value of 13.8 GPa (2.00×10^6 psi) and E:G of 16:1 (AF&PA 2001).
[3] Wood G_{13} values were estimated from G_{12}:G_{13} of 1.4:1.0.

Verification of torsional rigidity model

To optimize the placement of finite elements in the I-joist TDFIELD model, a convergence study was conducted using a series of isotropic and orthotropic rectangular sections. The numerically calculated torsional stiffness was compared to the corresponding theoretical solutions for GJ. The rectangular sections modeled were an isotropic aluminum member, a solid wood member assuming isotropic elasticity, and a solid wood member assuming orthotropic elasticity. The assumed G value of aluminum was 26.2 GPa (3.8×10^6 psi). The assumed modulus of elasticity of the wood members was13.8 GPa (2.0×10^6 psi); an E_1:G_{12} ratio of 16:1 was defined by the NDS (AF&PA 2001) A G_{12}:G_{13} ratio of 1.4:1 was chosen to model the orthotropic behavior of the wood composite materials observed from Janowiak et al. (2001). Table 2 shows the dimensions and shear moduli associated with each cross-section.

Element meshes took advantage of symmetry to model one-quarter of the cross-section with inclusion of appropriate boundary conditions. Three node triangular elements were specified. Uniform distributions of elements with a concentration of smaller elements near the midpoint of the larger side of the cross-section, where the torsional stresses are greatest in the member, were used. Selected uniform mesh arrangements included 3 nodes by 30 nodes, 3 by 38, 4 by 30, 4 by 38, 5 by 26, 5 by 30, 5 by 34, and 5 by 38 nodes. Selected concentrated meshes used uniform coarse meshes of 3 by 30 or 4 by 30 nodes coupled with a concentrated mesh of 8 by 8 nodes with heights of 0.64 cm (0.25-in.) and 0.32 cm (0.125-in.). Figure 4 shows the 0.32 cm (0.125-in.) 8 by 8 concentrated mesh with the 4 by 30 course mesh for the rectangular aluminum and solid wood sections.

Table 3 presents the results of the rectangular section TDFIELD GJ convergence study. The percentage difference values are shown for the comparison between the TDFIELD GJ and closed form solutions of Eqs. (4) and (5), as applicable. The isotropic aluminum section had minimum percent difference values of 0.97% for the 0.32-cm (0.125-in.) 8 by 8 node concentrated mesh with the 4 by 30 node coarse mesh. The isotropic wood section had minimum percent difference values of 1.88% for the 0.32-cm (0.125-in.) 8 by 8 node concentrated mesh with the 4 by 30 node coarse mesh. The orthotropic wood section had minimum percent difference values of 1.63% for the 0.32-cm (0.125-in.) 8 by 8 node concentrated mesh with the 4 by 30 node coarse mesh. Nodal concentrations at points of maximum stress increased the accuracy of the GJ prediction compared to the uniform node mesh. Of the mesh arrangements considered, the 0.32-cm (0.125-in.) 8 by 8 node concentrated mesh with the 4 by 30 node coarse mesh yielded the best results. Figure 4 shows the 0.32-cm (0.125-in.) 8 by 8 node concentrated mesh with the 4 by 30 node coarse mesh for both the aluminum and wood sections.

As a further confirmation of the adequacy of the TDFIELD finite element mesh used for the rectangular wood sections, the TDFIELD GJ predictions were compared with theoretical GJ predictions using Eqs. (4) and (5) with shear moduli

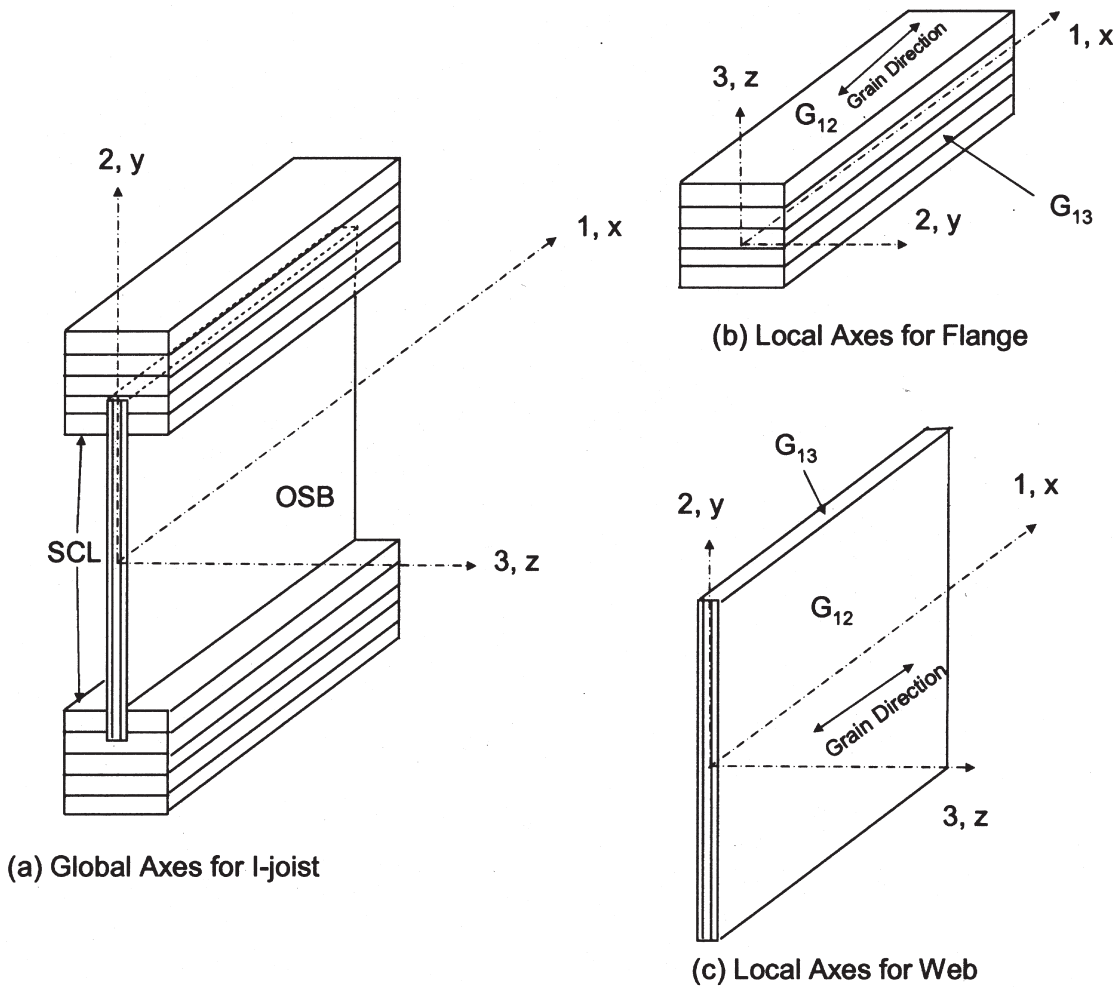

FIG. 4. Definition sketch of axes associated with I-joist section.

values from Hindman (2003). Table 4 gives the isotropic and orthotropic theoretical and TDFIELD GJ predictions including the percent difference. Percent difference values ranged from 1.3% to 1.8%, indicating that the TDFIELD model was repeatedly accurate in GJ predictions. The 0.32-cm (0.125-in.) 8 by 8 concentrated mesh near the neutral axis with the 4 by 30 coarse mesh was used for these calculations.

Figure 5(a) shows the global coordinate system associated with the composite I-joist section, while Fig. 5(b) shows the local coordinate system and shear moduli associated with the flange material, Fig. 5(c) shows the local coordinate system and shear moduli associated with the web material. Note that the global I-joist axes and local web axes correspond, whereas the global I-joist axes and local flange axes interchange the two- and three-directional axes.

Figure 6 shows the I-joist element mesh used to predict the GJ values using the TDFIELD program. The mesh represents one-quarter of the I-joist and contains 183 nodes and 288 triangular elements. Concentrations of nodes were placed at the points of high torsional stresses, namely the midpoint of each face of the I-joist. Concen-

TABLE 3. *Results of TDFIELD convergence study of rectangular materials.*

Type mesh[1]	Number of nodes	% Difference for aluminum isotropic section[2,3,4]	% Difference for wood isotropic section[2,3,4]	% Difference for wood orthotropic section[2,3,4]
Uniform	3 × 30	5.40	6.44	6.37
Uniform	3 × 38	5.40	6.49	6.43
Uniform	4 × 30	1.98	2.96	2.85
Uniform	4 × 38	1.94	2.97	2.87
Uniform	5 × 26	6.02	5.64	5.13
Uniform	5 × 30	6.07	6.62	6.36
Uniform	5 × 34	5.43	6.33	6.19
Uniform	5 × 38	4.87	5.92	5.83
Concentrated Mesh	0.64 cm (0.25 in) 8 × 8 Zone and 3 × 30	4.58	5.35	4.80
Concentrated Mesh	0.32 cm (0.125 in) 8 × 8 Zone and 3 × 30	5.03	4.74	4.17
Concentrated Mesh	0.64 cm (0.25 in) 8 × 8 Zone and 4 × 30	1.00	2.21	1.98
Concentrated Mesh	0.32 cm (0.125 in) 8 × 8 Zone and 4 × 30	0.97	1.88	1.63

[1] 'Uniform Mesh' used an equal spacing of nodes throughout the cross-section. 'Concentrated Mesh' used an 8 × 8 fine mesh near the location of greatest torsional stress.

[2] % Difference = 100 × [(Average Theoretical GJ – Average TDFIELD GJ)/Average Theoretical GJ]

[3] Aluminum and wood properties are defined in Table 2.

[4] Theoretical GJ values based on shear moduli from Table 2 and Equations 4 and 5 as appropriate.

TABLE 4. *TDFIELD torsional rigidity values for rectangular materials.*

Material	Elasticity	Average TDFIELD GJ N-m^2 (lb-in^2)[1]	Average theoretical GJ N-m^2 (lb-in^2)[2]	% Difference[3]
MSR Lumber	Isotropic	2.90×10^3 (1.01×10^6)	2.96×10^3 (1.03×10^6)	1.8
LVL	Isotropic	2.72×10^3 (9.48×10^5)	2.77×10^3 (9.65×10^5)	1.8
PSL	Isotropic	4.06×10^3 (1.41×10^6)	4.13×10^3 (1.44×10^6)	1.7
LSL	Isotropic	4.53×10^3 (1.58×10^6)	4.59×10^3 (1.60×10^6)	1.8
MSR Lumber	Orthotropic	2.77×10^3 (9.67×10^5)	2.85×10^3 (9.92×10^5)	1.4
LVL	Orthotropic	2.67×10^3 (9.31×10^5)	2.73×10^3 (9.52×10^5)	1.7
PSL	Orthotropic	3.96×10^3 (1.38×10^6)	4.05×10^3 (1.41×10^6)	1.5
LSL	Orthotropic	4.25×10^3 (1.48×10^6)	4.33×10^3 (1.51×10^6)	1.3

[1] TDFIELD GJ terms were determined using the TDFIELD finite element program with 0.32 cm (0.125 in) 8 by 8 concentrated mesh and 4 by 30 coarse mesh.

[2] Theoretical GJ terms were determined from Equations 4 for isotropic elasticity and Equation 5 for orthotropic elasticity using shear modulus values from Hindman et al. (2004a).

[3] % Difference = ((Average Theoretical GJ – Average TDFIELD GJ)/Average Theoretical GJ) × 100.

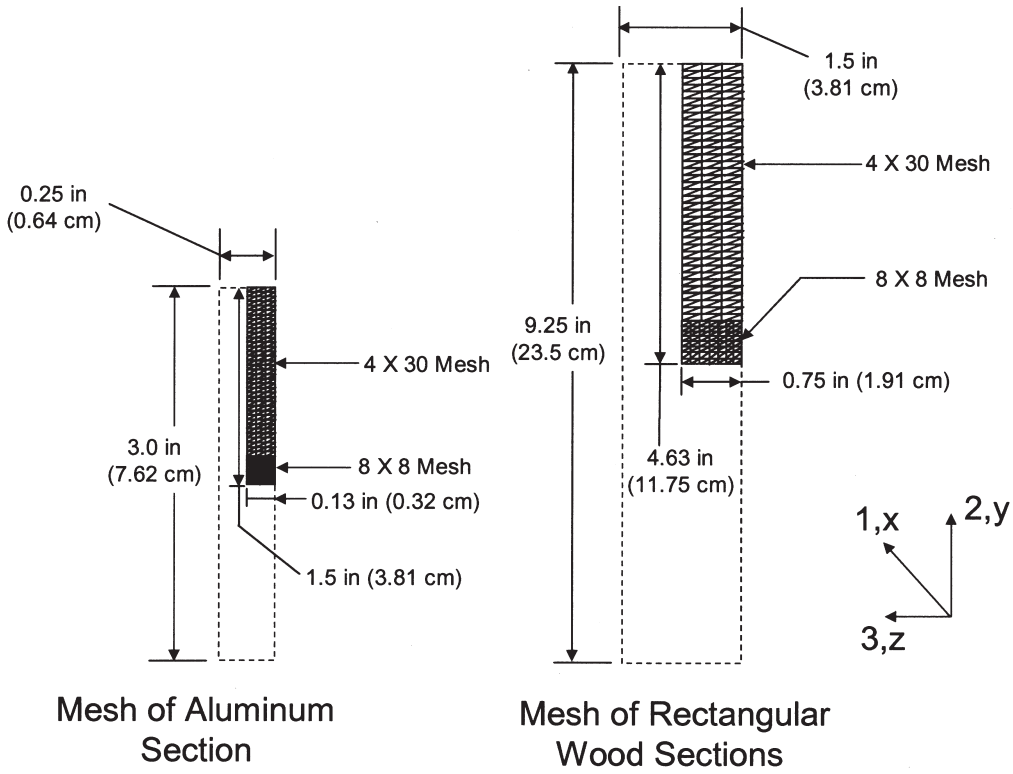

FIG. 5. Best element mesh of aluminum and wood sections from convergence study.

trations of nodes were also placed around the perimeter of the flange and at the connection between the flange and web. The web-flange connection was modeled as a rigid connection based on previous work by Fridley and Tang (1992), who reported negligible slip in an I-joist web-flange connection under bending loading.

Predictions of torsional rigidity and comparison to experimental values

The test material torsional rigidity values were predicted based upon previously determined elastic constants from Hindman et al. (2005b). To provide a statistical comparison of the predicted and measured torsional rigidity values, the 95% confidence intervals (CI) of the measured torsional rigidity terms were compared with the upper and lower bounds of the predicted torsional rigidity terms resulting from the use of the 95% CI values of the shear moduli terms. Table 5 shows the average and the upper and lower 95% CI values for G_{12} and G_{13} (Hindman et al. 2005b). These shear moduli were experimentally measured on separate matched material samples using the five-point bending test described in Hindman (2003).

Three different sets of shear moduli values were coupled with the element mesh described above for I-joist GJ prediction. First, isotropic elasticity assumptions used the G_{12} values of both flange and web materials. However, this isotropic elasticity assumption may not be accurate since the 1–3 plane of the flange and 1–2 plane of the web are in the 1–2 plane of the I-joist (Figure 4). Therefore, another isotropic elasticity assumption, called the 'mixed' isotropic elasticity, incorporating the G_{13} of the flange and G_{12} of the web was investigated. Finally, an orthotropic elasticity assumption, using the respective G_{12} and G_{13} values of the web and flange, was investigated.

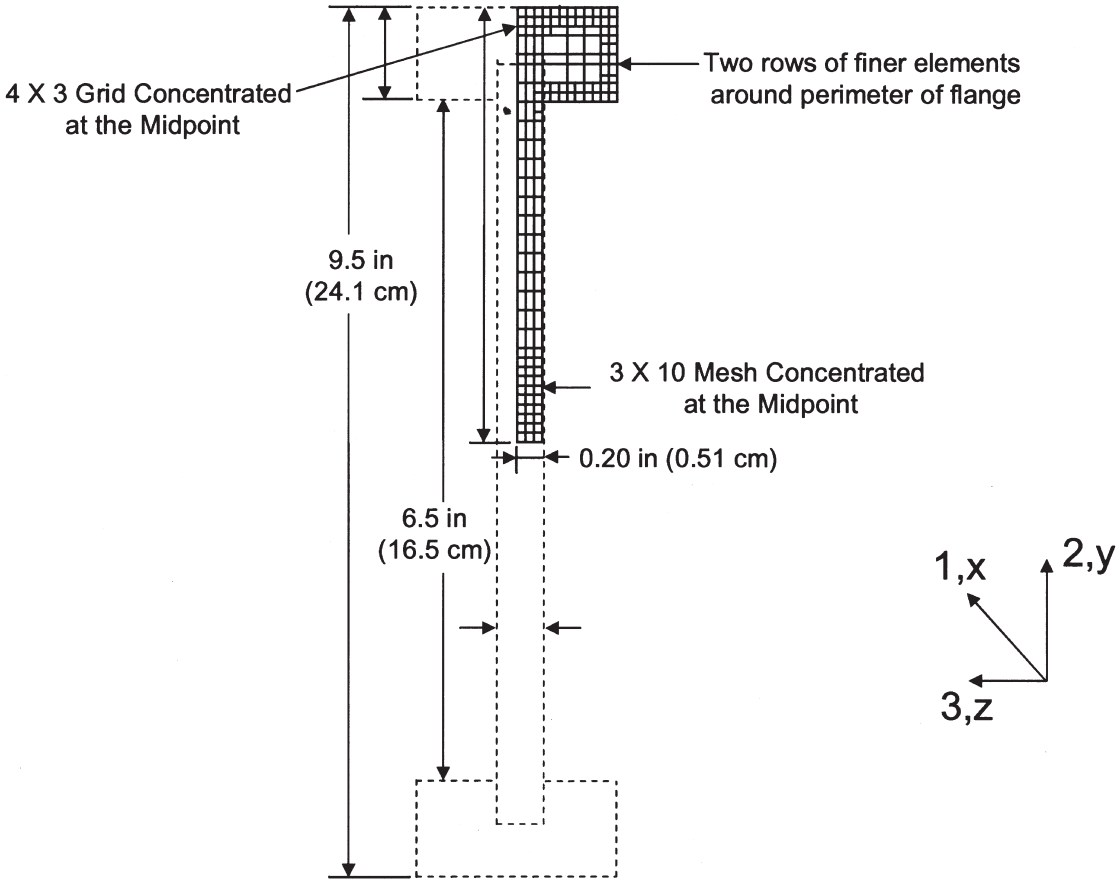

FIG. 6. Element Mesh of I-joist Used for TDFIELD Solution.

RESULTS AND DISUCSSION

Summary data collection

Table 6 shows the effective length, measured torsional rigidity and COV values for the materials tested. The effective length term is based upon the original gage length of 147 cm (58 in.) and the ELD adjustment. The ELD adjustment lowered the effective length to 121.4 cm (47.8 in.) for the LVL I-joist and 125 cm (49.2 in.) for the LSL I-joist, showing some variation in the equivalent length term by I-joist configuration. The COVs of the I-joist material GJ were both less than 10%. The LVL I-joist GJ value was 2.3% less than the LSL I-joist GJ value, even though the two I-joists have different flange widths (the LVL flange width was 3.81 cm (1.5 in.); LSL flange width was 4.45 cm (1.75 in.)). The change in flange width seems to account for the lower shear modulus of the LSL material (Hindman et al. 2005a) to produce a torsional rigidity nearly equivalent to the LVL I-joist value.

Comparative analysis of observed torsional rigidity

An analysis of variance was conducted to determine if statistical differences existed between the GJ values from the two I-joist materials. Two factors were analyzed in the ANOVA—a material factor and a specimen factor. The material factor examined the differences between the GJ values of the two I-joist materials. The material factor p-value was 0.367, indicating there was no

TABLE 5. *The 95% confidence intervals of shear moduli (Hindman et al., 2004a).*

	G_{12}			G_{13}		
Material	Lower CI MPa (psi)	Average MPa (psi)	Upper CI MPa (psi)	Lower CI MPa (psi)	Average MPa (psi)	Upper CI MPa (psi)
LVL	679 (9.85×10^4)	710 (1.03×10^5)	745 (1.08×10^5)	514 (7.46×10^4)	54.9 (7.96×10^4)	58.3 (8.46×10^4)
LSL	965 (1.40×10^5)	1040 (1.51×10^5)	1110 (1.61×10^5)	409 (5.93×10^4)	436 (6.32×10^4)	463 (6.71×10^4)
OSB	595 (8.63×10^4)	678 (9.83×10^4)	758 (1.10×10^5)	20.3 (2.95×10^3)	25.9 (3.75×10^3)	31.4 (4.55×10^3)

TABLE 6. *Experimental torsional rigidity (GJ) values.*

Material	Effective Length, cm (in)[1]	Torsional Rigidity (GJ)[2] N-m² (lb-in²)	COV %
LVL I-joist	121 (47.8)	637 (2.22 $\times 10^5$)	7.2
LSL I-joist	125 (49.2)	651 (2.27 $\times 10^5$)	4.4

[1] Effective length determination procedures are described in Hindman (2003).

[2] Sixteen specimens with three loading repetitions were tested for each material.

significant difference between the two materials. The specimen factor examined differences in the GJ values from the 16 specimens of each I-joist material. The specimen factor p-value was 0.598, indicating that the GJ values from the different specimens were not significantly different. Therefore, the measured GJ values of the two I-joists are equal.

Experimental vs. predicted torsional rigidity

Table 7 shows the average GJ predictions and the percent difference values compared to the measured GJ results from Table 5. The average isotropic GJ predictions were greater than the measured GJ predictions and the average orthotropic GJ predictions were less than the measured GJ predictions. The mixed isotropic GJ prediction, using G_{13} of the flange and G_{12} of the web, produced GJ predictions less than 10% different than the measured GJ values. Because of the higher torsional stresses and strains present on the larger cross-sectional face of the specimen, the shear moduli terms (G_{13} of the flange and G_{12} of the web) associated with this face dominate the torsional rigidity prediction of the I-joist cross-section.

Figure 7 shows the 95% CI values of the measured GJ terms and the prediction bounds of the different GJ predictions. The mixed isotropic GJ prediction overlapped both the LVL I-joist and LSL I-joist measured GJ 95% CI, respectively. Isotropic GJ estimations for both I-joist materials were much greater than the measured results. The orthotropic GJ prediction of the LSL I-joist overlaps the measured 95% CI values, while the LVL I-joist orthotropic GJ prediction does not.

TABLE 7. *Experimental and predicted torsional rigidity values.*

Material	Prediction	GJ, N-m² (lb-in²)	% Difference from experimental[1,2]
LVL I-joist	Isotropic GJ3	743 (2.59 × 105)	116.6
LVL I-joist	Orthotropic GJ[4]	447 (1.56 × 10^5)	–29.8
LVL I-joist	Isotropic Mixed GJ[5]	602 (2.10 × 10^5)	-5.5
LSL I-joist	Isotropic GJ	1300 (4.53 × 10^5)	+99.6
LSL I-joist	Orthotropic GJ	585 (2.04 × 10^5)	–10.1
LSL I-joist	Isotropic Mixed GJ[3]	637 (2.22 × 10^5)	–2.1

[1] % Difference = (Prediction-Experimental)/Experimental) × 100.

[2] Experimental values given in Table 5.

4 Orthotropic GJ uses both the G12 and G13 values of the web and flange.

[5] Isotropic Mixed GJ uses the G_{12} of the web and G_{13} of the flange.

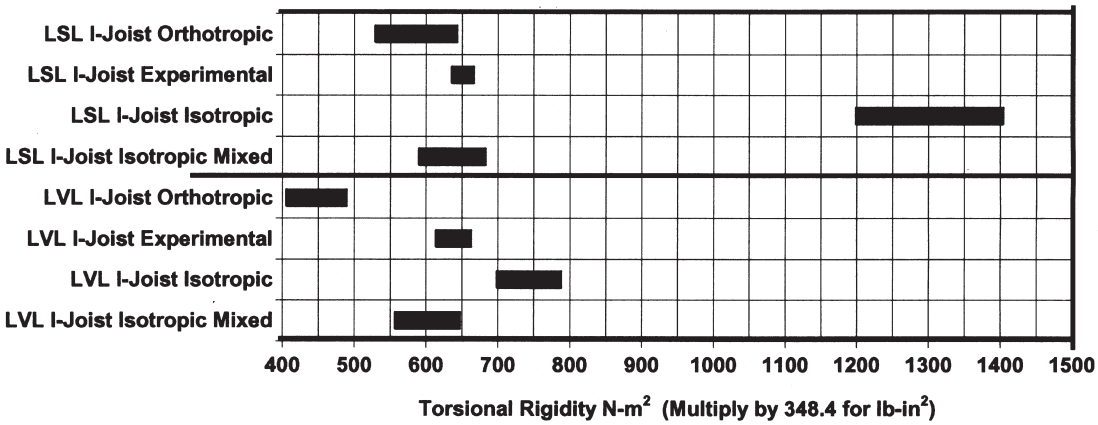

FIG. 7. Torsional rigidity confidence intervals for I-joist materials.

Interestingly, the LVL I-joist mixed isotropic GJ prediction overlaps the LSL I-joist mixed isotropic GJ prediction. The mixed isotropic GJ prediction indicates that the planar shear moduli in the larger cross-sectional dimension have a greater effect upon the GJ results as compared to the isotropic or orthotropic shear moduli. For prediction of the measured GJ values for I-joists, the most important elastic constants are the edgewise G_{12} of the web material and the flatwise G_{13} of the flange material.

Examination of current design predictions vs. best fit prediction of torsional rigidity

After the best fit prediction equations for the GJ of each I-joist were determined, the GJ predictions were examined to determine if they represent changes compared to the common assumption of an E:G ratio of 16:1 for wood materials. The GJ of each I-joist section was predicted using the TDFIELD program and isotropic shear moduli values for the web and flange materials based upon the assumed E:G ratio of 16:1 (AF&PA 2001). Table 8 shows the resultant GJ predictions and the percent difference of the best fit predictions compared to those using the assumed E:G ratio of 16:1. Compared to calculated GJs assuming E:G = 16:1, the best fit models using measured shear moduli were 33.2% lower for the LVL I-joist and 29.3% lower for the LSL I-joist. If the assumed E:G ratio for GJ prediction was used, the result would be a 30% increase in the GJ value compared to the best fit predictions and experimentally measured results of this study. This demonstrates the importance of using the actual G_{ij} and E:G ratios of the individual I-joist components to obtain accurate predictions of I-joist torsional stiffness.

CONCLUSIONS

The torsional rigidity of two different I-joist materials was measured and then predicted using the planar shear moduli and the TDFIELD finite element program. The GJ values measured for the LVL I-joist and LSL I-joist were not significantly different despite different flange materials and flange widths. Predictions of the torsional rigidity used an element mesh with concentrated nodes at the midpoint of the beam and around the flange perimeter. Three different sets of elas-

TABLE 8. *Prediction of torsional rigidity for I-joist members using current and revised prediction methods.*

Material	GJ from E:G = 16:1 N-m^2 (lb-in^2)	Best GJ Predictions[1] N-m^2 (lb-in^2)	% Difference[2]
LVL I-joist[3]	901 (3.14×10^5)	602 (2.10×10^5)	–33.2%
LSL I-joist[3]	901 (3.14×10^5)	637 (2.22×10^5)	–29.3%

[1] Best GJ predictions for LVL I-joist and LSL I-joist were the Isotropic Mixed GJ from Table 7.

[2] % Difference = (Best GJ Prediction – GJ from E:G = 16.0)/GJ from E:G = 16.0) X 100

[3] Cross-section of I-joists defined in Table 1 and Figure 1.

tic constant ratios were used – isotropic G_{12} values, orthotropic G_{12} and G_{13} values and mixed isotropic values with G_{12} of the web and G_{13} of the flange. The mixed isotropic GJ prediction provided closer agreement than the isotropic or orthotropic GJ predictions. The planar shear moduli in the larger dimension of the I-joist section, namely the G_{12} of the web and the G_{13} of the flange, are recommended in the prediction of torsional rigidity of I-joist materials. The shear moduli associated with the components of the I-joist should be used for GJ calculation rather than assuming an E:G ratio of 16:1.

ACKNOWLEDGMENTS

The authors would like to thank Trus Joist, a Weyerhaeuser company, Rigidply Rafters, the Pennsylvania Housing Research Center and the Pennsylvania Agricultural Experiment Station for material donations and support for this project.

REFERENCES

AF&PA. 2001. Allowable stress design (ASD) manual for engineered wood construction. American Forest and Paper Association. Washington, D.C. 700 pp.

Cook, R. D. and W. C. Young. 1985. Advanced mechanics of materials. Prentice Hall, Inc., Upper Saddle River, NJ. 539 pp.

Fridley, K. J., and R. C. Tang. 1992. Shear effects on the creep behavior of wood composite I-beams. Forest Prod. J. 42(6):17–22.

Hindman, D. P. 2003. Torsional rigidity and lateral stability of structural composite lumber and I-joist members. Ph.D. Dissertation, The Pennsylvania State University, University Park, PA, 222 pp.

———, H. B. Manbeck, J. J. Janowiak. 2005a. Torsional rigidity of rectangular wood composite materials. Wood Fiber Sci. Submitted for publication.

———, ———, and ———. 2005b. Comparison of ASTM D 198 and five-point bending for elastic constant ratio determination. Forest Prod. J. Submitted for publication.

Janowiak, J. J., D. P. Hindman, H. B. Manbeck. 2001. Orthotropic behavior of lumber composite materials. *Wood and Fiber Sci.* 33(4):580–594.

Lekhnitskii, S. G. 1963. Theory of elasticity of an anisotropic elastic body. Translated by P. Fern, Edited by J. J. Brandstatter. Holden-Day, Inc., San Francisco, CA. USA.

Segerlind, L. J. 1984. Applied finite element analysis. 2nd edition. John Wiley and Sons, New York, NY. 427 pp.

Tarnopol'skii, Y. M. and T. Kincis. 1985. Static test methods for composites. Van Nostrand Reinhold Company. New York, NY 301 pp.

Timoshenko, S. and J. N. Goodier. 1951. Theory of elasticity. 2nd edition. McGraw-Hill, New York, NY. 506 pp.